Nigrostriatal α-synucleinopathy induced by viral vector-mediated overexpression of human α-synuclein: A new primate model of Parkinson's disease

Deniz Kirik*†, Lucy E. Annett‡, Corinna Burger§¶, Nicholas Muzyczka§¶, Ronald J. Mandel¶‖, and Anders Björklund*

*Wallenberg Neuroscience Center, Department of Physiological Sciences, Division of Neurobiology, Lund University, BMC A11, 221 84 Lund, Sweden; ‡Psychology Department, University of Hertfordshire, College Lane, Hatfield, Hertfordshire AL10 9AB, United Kingdom; and §Department of Molecular Genetics and Microbiology, and ‖Department of Neuroscience, McKnight Brain Institute, and ¶Powell Gene Therapy Center, University of Florida, P.O. Box 100244, Gainesville, FL 32610

Edited by Ann M. Graybiel, Massachusetts Institute of Technology, Cambridge, MA, and approved January 7, 2003 (received for review October 21, 2002)

We used a high-titer recombinant adeno-associated virus (rAAV) vector to express WT or mutant human α-synuclein in the substantia nigra of adult marmosets. The α-synuclein protein was expressed in 90–95% of all nigral dopamine neurons and distributed by anterograde transport throughout their axonal and dendritic projections. The transduced neurons developed severe neuronal pathology, including α-synuclein-positive cytoplasmic inclusions and granular deposits; swollen, dystrophic, and fragmented neuritis; and shrunken and pyknotic, densely α-synuclein-positive perikarya. By 16 wk posttransduction, 30–60% of the tyrosine hydroxylase-positive neurons were lost, and the tyrosine hydroxylase-positive innervation of the caudate nucleus and putamen was reduced to a similar extent. The rAAV-α-synuclein-treated monkeys developed a type of motor impairment, i.e., head position bias, compatible with this magnitude of nigrostriatal damage. rAAV vector-mediated α-synuclein gene transfer provides a transgenic primate model of nigrostriatal α-synucleinopathy that is of particular interest because it develops slowly over time, like human Parkinson's disease (PD), and expresses neuropathological features (α-synuclein-positive inclusions and dystrophic neurites, in particular) that are similar to those seen in idiopathic PD. This model offers new opportunities for the study of pathogenetic mechanisms and exploration of new therapeutic targets of particular relevance to human PD.

Dopamine neurodegeneration induced by MPTP (1-methyl-4-phenyl-1,2,3,6-tetrahydropyridine) is currently the best available primate model of Parkinson's disease (PD; see refs. 1 and 2 for a current review). In adult monkeys, MPTP administration induces profound loss of dopamine neurons in the substantia nigra (SN) and motor impairments similar to those seen in idiopathic PD. The MPTP model, however, has two obvious limitations. First, MPTP-induced toxicity is a rapid, single-hit event, resulting in an acute onset of neurodegeneration and neurological symptoms. Second, the MPTP-affected dopamine neurons do not develop the progressive α-synucleinopathy (Lewy bodies and Lewy neuritis, in particular) that is the characteristic hallmark of idiopathic PD. There is thus an obvious need for a new primate model of PD where the pathogenetic mechanisms associated with α-synuclein (α-syn) toxicity and nigrostriatal degeneration can be studied in species close to man.

Previous studies have shown that the α-syn protein is a major component of the intraneuronal protein aggregates (Lewy bodies and Lewy neuritis) that are pathological hallmarks of the disease (3, 4). Moreover, point mutations in the α-syn gene have been shown to cause familiar PD (5, 6), suggesting that abnormal processing and/or function of α-syn may trigger the neurodegenerative process. Although α-syn is expressed in neurons throughout the nervous system, neurodegeneration in PD is remarkably selective and is most prominent in the dopaminergic neurons of the SN. Recent studies suggest that this selective vulnerability may be due to interaction of α-syn with intracellular dopamine, oxidative stress, and dopamine-dependent free radical damage (7–10). This interaction probably explains why dopaminergic neurons are affected by α-syn at expression levels that are nontoxic to other types of cells (10–13).

These *in vitro* data raise the possibility of generating transgenic models of PD by overexpression of the α-syn protein in the nigrostriatal dopamine neurons. This approach has given promising results in *Drosophila* (14). Nevertheless, the attempts made so far in mice, by using standard transgenic technology, have been disappointing. In the transgenic mouse strains generated to date, WT or mutated human α-syn have been expressed under neuron-specific promoters; although α-syn accumulation, α-syn-positive inclusions, and signs of neuronal injury have been widespread, no significant nigral pathology or cell loss has been detected in any of these mice (15–21). Recently, however, direct gene transfer by means of viral vectors has emerged as an interesting alternative to the standard transgenic approach. Recombinant adeno-associated virus (rAAV) and lentivirus vectors, in particular, are useful for this purpose because they transduce nondividing neurons with high efficiency in the CNS and are integrated and stably expressed without any signs of inflammatory or immune reactions (22, 23). These vector systems can be targeted to specific subregions of the CNS, and, in contrast to standard transgenic technology, they offer a transgenic approach that can be applied in adult animals and in other species than mice, such as rats and primates.

The rAAV vectors are of special interest in the context of PD because of their exceptionally high affinity for nigral dopamine neurons. In a previous study (24), we have shown that the rAAV vector system can be used to overexpress WT or mutant α-syn in the nigrostriatal neurons in adult rats, and that this overexpression is accompanied by the development of a pronounced α-synucleinopathy, including the appearance of α-syn-positive cytoplasmic inclusions and dystrophic neurites, a gradual loss of 30–80% of the nigral dopamine neurons, and PD-like behavioral improvements.

In the present study, we have applied this rAAV-α-syn vector construct to express human α-syn in the nigrostriatal dopamine neurons in a small nonhuman primate, the common marmoset. We report that the rAAV vector is equally effective in transducing the pars compacta neurons of the primate SN and show that overexpression of either WT or mutant human α-syn is sufficient to induce a PD-like neuropathology in the primate

This paper was submitted directly (Track II) to the PNAS office.

Abbreviations: MPTP, 1-methyl-4-phenyl-1,2,3,6-tetrahydropyridine; PD, Parkinson's disease; SN, substantia nigra; α-syn, α-synuclein; rAAV, recombinant adeno-associated virus; TH, tyrosine hydroxylase; VMAT-2, vesicular monoamine transporter-2; VTA, ventral tegmental area.

†To whom correspondence should be addressed. E-mail: deniz.kirik@mphy.lu.se.

 www.pnas.org/cgi/doi/10.1073/pnas.0536383100

nigrostriatal system, accompanied by dopamine neuron cell loss and signs of motor impairments.

Experimental Protocols

rAAV Vectors. The rAAV-CBA-α-syn, rAAV-CBA-mu-α-syn, and rAAV-CBA-GFP vectors were produced by using a double transfection method with rAAV plasmids and a helper plasmid containing the necessary gene products normally provided by adenovirus (25), and purified as described (26). The final titers were 8.2×10^{11}, 1.4×10^{12}, and 1.5×10^{11} infectious units/ml, respectively, for the three vectors, as determined by an infectious center assay (27). The vectors express the transgene from a hybrid promoter consisting of an enhancer element from the cytomegalovirus promoter, followed by the chicken β-actin promoter containing a rabbit β-globin intron, termed CBA (28).

Animals and Surgery. All procedures were carried out under a project license in accord with the U.K. Animals (Scientific Procedures) Act 1986. Eight adult common marmosets (*Callithrix jacchus),* four males and four females, were used. All were laboratory-bred, aged 65–72 mo and weighed 340–380 g at the start of the experiment. The monkeys were housed in pairs with both members of the pair receiving the same type of rAAV vector injection. Two monkeys received injections of the rAAV vectors encoding the WT human α-syn, two received A53T mutated human α-syn, and four received a control vector encoding the GFP. In one of the rAAV-wt-α-syn injected animals, the injections failed; this animal was not included in the further analysis.

For surgery, the marmosets were anesthetized with alphaxalone-alphadone (Saffan; Schering–Plough; 0.5 ml of 12 mg/ml, i.m.). A supplementary dose of 0.3 ml Saffan was given during surgery if necessary. Infusions of 3 μl rAAV were made unilaterally at each of two sites in the right SN: anterior (A) 5.5, lateral (L) −2.5, and ventral (V) 6.6; and A 4.0, L −2.5, and V 6.6 [coordinates derived from the stereotaxic atlas of Stephan *et al.* (29)]. The injections were made at a rate of 0.25 μl/min by using a 29-gauge injection needle that was left in place for a further 4 min after each injection. After surgery, the monkeys were given an analgesic (Finadyne, Schering–Plough; 0.1 mg/kg, s.c.) and kept warm in an incubator until well enough to be returned to their home cage, usually later that day.

Behavior. Changes in motor behavior over time were monitored by amphetamine-induced rotation and a head position bias test (30, 31). In the latter test, the direction of the head relative to the body axis (ipsi- or contralateral to the injected side or straight ahead) was scored every second over three 1-min periods. The time difference (ipsi–contra) was used as a measure of head position bias. Tests were conducted preoperatively, at three weekly intervals and 16 wk after the AAV infusions.

Histology. The monkeys were perfused for histological analysis at 3–16 wk after vector injection. After premedication with 0.05 ml ketamine (Vetalar; Shering–Plough; 100 mg/ml, i.m.) and under deep anesthesia with 0.8 ml of sodium pentobarbitone (200 mg/ml, i.p.), the monkeys were perfused transcardially with 300 ml PBS, followed by 1,000 ml of 4% paraformaldehyde in PBS. The brains were placed in 4% paraformaldehyde solution for 24 h, after which they were transferred to 30% sucrose solution in PBS. Immunohistochemical stainings were performed on free-floating sections by using antibodies raised against tyrosine hydroxylase (TH; rabbit IgG, 1:250, Pel-Freez Biologicals), GFP (rabbit IgG, 1:20,000, Abcam, Cambridge, U.K.), vesicular monoamine transporter-2 (VMAT-2; rabbit IgG, 1:2,000, Chemicon), Hu (mouse IgG, 1:1,000, courtesy of S. A. Goldman, Cornell University, Ithaca, NY), and human α-syn (mouse IgG, 1:16,000, courtesy of V. M. Lee, University of Pennsylvania, Philadelphia). Incubation with primary antibodies was followed with the appropriate secondary antibodies conjugated to biotin, and avidin-biotin-peroxidase complex (ABC Elite, Vector Laboratories), visualized with 3,3′-diaminobenzidine, mounted on chrome-alum-coated glass slides and coverslipped. For colocalization of GFP and TH, incubation with anti-TH primary antibody was followed by donkey anti-rabbit antibody conjugated to Cy3 (red), and GFP was visualized using confocal microscopy by its native fluorescence in the green channel. An additional series of sections were stained for cresyl violet.

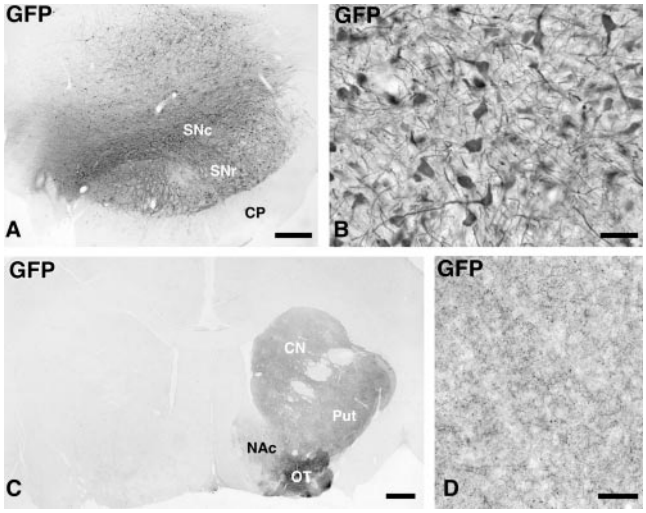

Fig. 1. Photomicrographs showing the expression of the GFP transgene in monkeys injected with the control vector. (*A* and *B*) GFP was expressed in the vast majority of the neurons in SN pars compacta, and some cells dorsally in the mesephalic tegmentum and ventrally in the SN pars reticulata (*A*). The transgenic GFP protein was transported along the axons of the nigrostriatal projection system to the caudate nucleus, putamen, and lateral olfactory tubercle, whereas the projections to the medial olfactory tubercle and the nc. accumbens were not labeled to the same extent (*C*; the noninjected control side is to the left). The density of GFP-expressing fibers in the striatum is shown in *D*. Scale bar in *A* = 0.5 mm; *B* and *D* = 50; *C* = 1 mm.

The total number of TH-positive and VMAT-2-positive neurons in the SN were estimated in separate series of sections according to the optical fractionator principle (32), by using the Olympus CAST system (Olympus Denmark A/S, Albertslund, Denmark). Every eighth section covering the entire extent of the SN was included in the counting procedure. The borders of the SN were defined as follows: the medial border between the ventral tegmental cell group and the pars compacta region was just lateral to the roots of the third nerve. At the most caudal level, the pars compacta was defined as the dense TH cell group ventral to the medial lemniscus and the retrorubral area. The TH-positive cells in the pars retriculata (and therefore dorsal to the cerebral peduncle) were included in the cell counts. This definition led typically to seven to eight sections per monkey being measured. A coefficient of error of <0.10 due to the estimation was accepted.

Results

The animals received injections of high-titer rAAV-α-syn and rAAV-GFP vectors unilaterally at two sites (2×3 μl) in the SN and were perfused at 3 wk ($n = 2$ from GFP group), and 16 wk ($n = 3$ from α-syn group and $n = 2$ from GFP group) after the transduction. In the rAAV-GFP-injected animals, 90–95% of the TH-positive cells were found to express GFP at all rostrocaudal levels throughout the SN, indicating that the nigral dopamine neurons were very efficiently transduced in the marmoset brain (Fig. 1 *A* and *B*). Most of the transduced cells in the

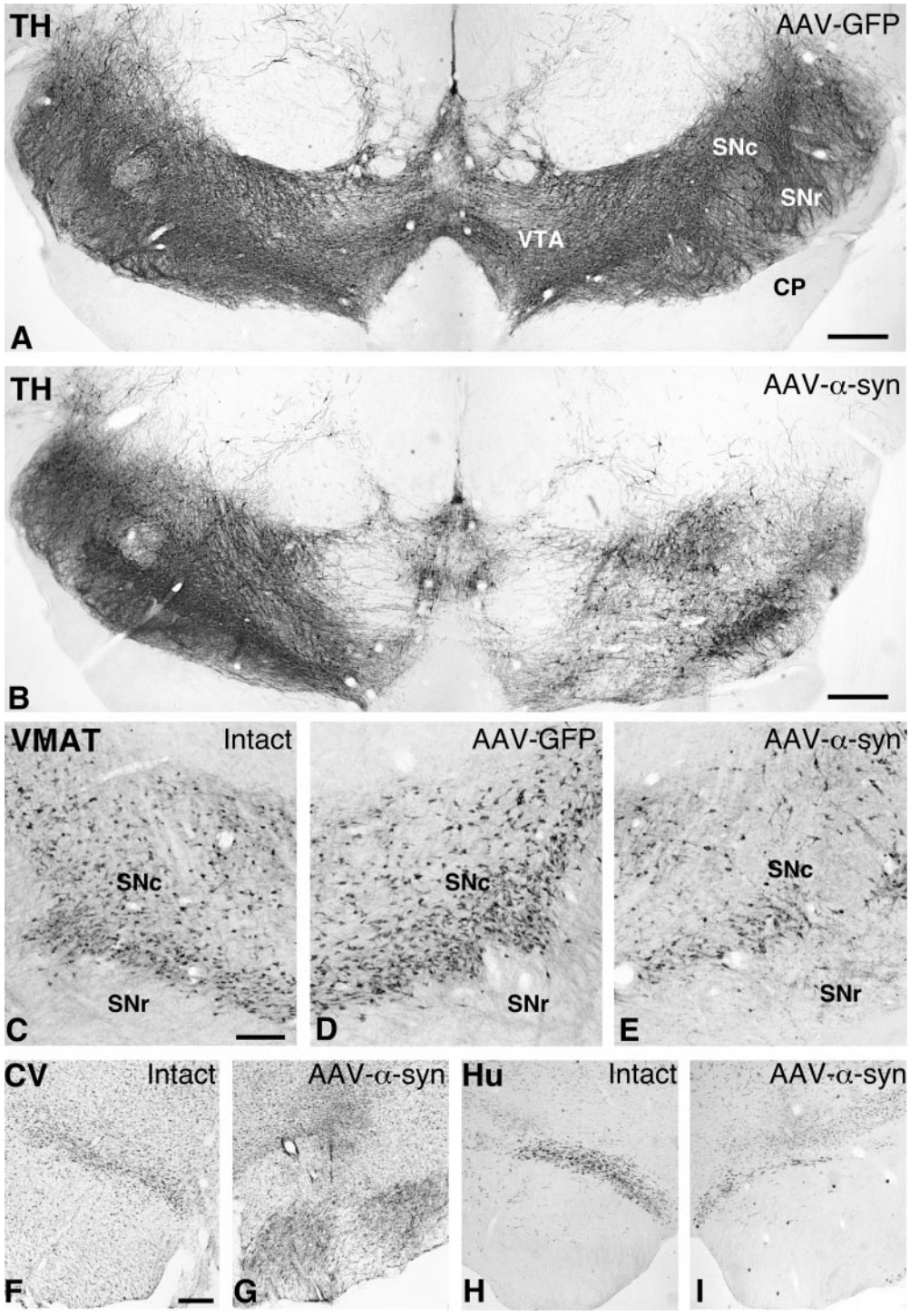

Fig. 2. Photomicrographs showing the TH-stained (*A* and *B*), VMAT-2-stained (*C–E*), cresyl violet-stained (*F* and *G*), and Hu-stained (*H* and *I*) sections at the level of SN. In the rAAV-GFP-treated animals, both TH (*A*) and VMAT (compare *C* and *D*) staining showed normal numbers and distribution of nigral dopaminergic cells. In the rAAV-α-syn-injected animals, by contrast, a clear loss of cells was seen both with TH (*B*) and VMAT-2 stainings (compare *C* and *E*). Scale bars in *A* and *B* = 0.5 mm; *C* = 300 μm (applies to *C–E*); *F* = 300 μm (applies to *F–I*). CP, cerebral peduncle; SNc, substantia nigra pars compacta; SNr, substantia nigra pars reticulate; VTA, ventral tegmental area.

SN were confined to the pars compacta, but some GFP-expressing cells were also found in the ventral tegmental area (VTA). In addition, GFP-expressing cells occurred in the SN pars reticulata, ventral to TH-positive cells, and dorsally in the mesencephalic tegmentum (Fig. 1*A*). In the two animals killed at 3 wk after rAAV-GFP injection, transgene expression was confined to the cell bodies and proximal axons within the SN pars compacta, as well as the dendrites extending into the pars reticulata. At 16 wk, transgene expression was maintained at a high level in the SN. In addition, anterogradely transported GFP protein could now be visualized also along the entire nigrostriatal pathway and in axon terminals throughout the striatum,

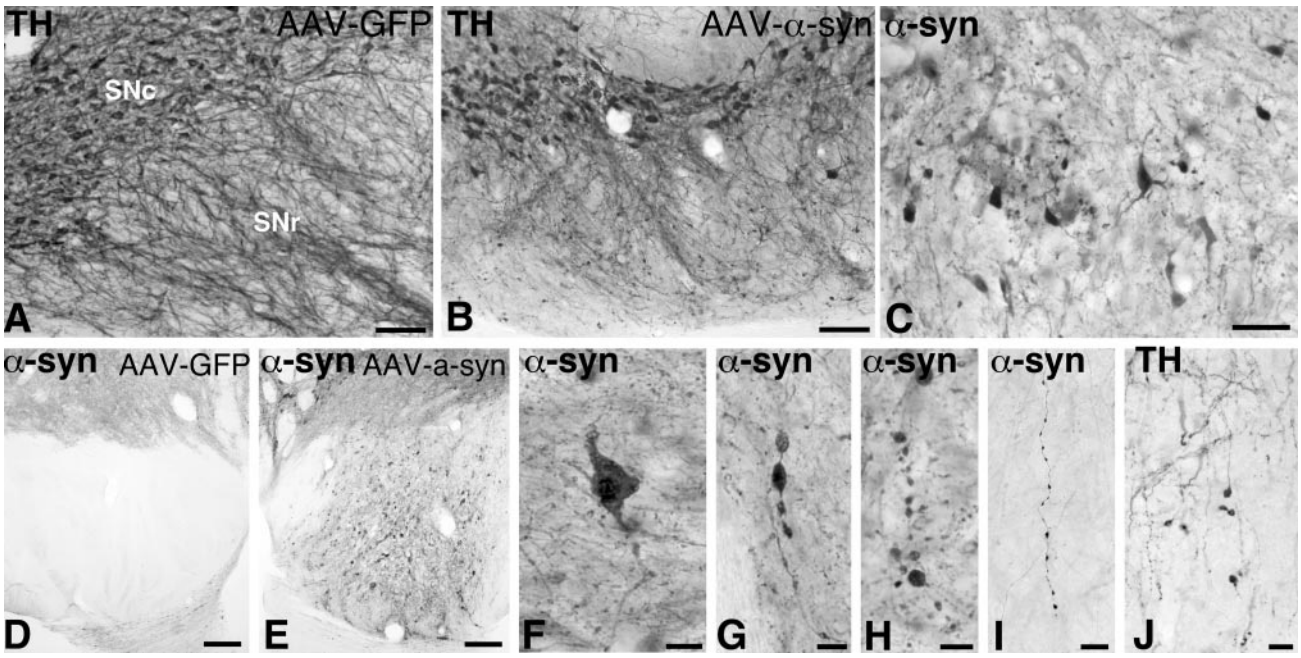

Fig. 3. Nigral degeneration in the rAAV-α-syn-injected animals. Pathological profiles in the SN were seen both with TH (*A*, *B*, and *J*) and α-syn immunoreactivity (*C–I*). Extensive cellular degeneration in the SN pars compacta, as visualized by TH immunoreactivity, also led to prominent dendritic abnormalities and loss of dendrites in the SN pars reticulata (*B* and *J*). Affected but surviving cells in SN pars compacta were shrunken (*C*) and contained numerous inclusions within the cytoplasm and proximal neurites (*F*), as well as in axons within pars compacta (*G* and *H*) and along the nigrostriatal bundle (*I*). Numerous pathological fibers with prominent inclusions were observed in the cerebral puduncle (cf. *D* and *E*). Scale bars in *A* and *B* = 0.1 mm; *C*, *I*, and *J* = 50 μm; *D* and *E* = 0.2 mm; *F*, *G*, and *H* = 25 μm.

including nc. accumbens and olfactory tubercle (Fig. 1 *C* and *D*). No signs of damage or degeneration could be detected in the GFP-transduced cells or their processes with any of the markers used (TH, VMAT-2, Hu, and cresyl violet; data not shown).

In animals injected with either of the two α-syn vectors, by contrast, there were clear signs of degeneration in the nigrostriatal dopamine neurons. The total number of TH-positive cells in the injected SN, as determined by stereology, was decreased by 32–61% in the three injected animals (from an average of 47,106 cells on the contralateral untreated side, to an average of 26,797 on the injected side; cf. Fig. 2 *A* and *B*). The same magnitude of cell loss (41–62%; from 43,034 cells on the control side to 23,214 cells on the injected side) was observed also in sections stained for the vesicular monoamine transporter, VMAT-2, arguing against the possibility of a selective down-regulation of TH protein in the α-syn-expressing cells (Fig. 2 *C–E*). The loss of dopaminergic cells was further supported by a similar reduction in the number of neuronal profiles within SN pars compacta in sections stained for the pan-neuronal marker, Hu, or with cresyl violet (Fig. 2 *F–I*). Cell death was most prominent in the central part of the SN but was seen at all rostrocaudal levels. Loss of TH- and VMAT-2-positive cells was observed also in the VTA, although of lesser magnitude than in SN. No such cell loss was observed in any of the rAAV-GFP-treated control monkeys (Fig. 2*A*).

Close examination of the SN transduced with either WT or mutant α-syn revealed signs of degeneration and ongoing pathology in the neurons of the pars compacta, including α-syn-positive cytoplasmic inclusions and granular deposits (Fig. 3*F*), α-syn- and TH-positive swollen, dystrophic and fragmented neurites (Fig. 3 *C*, *G*, and *H*), and shrunken, pyknotic perikarya with dense α-syn immunoreactivity (Fig. 3 *B* and *C*). Also, the dendrites projecting into the pars reticulata were severely damaged (cf. Fig. 3 *A*, *B*, and *J*), and α-syn- and TH-positive inclusions and swollen axons could be traced in large numbers along the nigrostriatal pathway (Fig. 3 *D* and *E*). Many of the surviving nigral cells, however, still expressing α-syn, had a normal intact appearance (Fig. 3*B*). In these cells, the α-syn immunoreactivity had an even, diffuse cytoplasmic distribution, suggesting that they had escaped the α-syn-induced toxic impact.

In the rAAV-α-syn-injected monkeys, degenerative changes in the axon terminals in the striatum could be visualized both with TH (Fig. 4*C*) and VMAT-2 antibodies (Fig. 4*D*). None of these changes were seen in the animals injected with the rAAV-GFP control vector (Fig. 4 *A* and *B*). A substantial loss of TH- and VMAT-2-positive fibers, in the order of 40–50%, occurred throughout the caudate nucleus and putamen, whereas the innervation in the ventral striatal and limbic regions, including nc. accumbens and the olfactory tubercle, was relatively spared (Fig. 4*C*; cf. Fig. 4 *E* and *F*). Swollen axons and pathological inclusions were observed in the remaining sparse TH-positive innervation in the striatum (Fig. 4 *F* and *G*), and also within the internal capsule (not shown).

In the behavioral tests, amphetamine-induced rotation did not show any consistent changes at any time point (data not shown). In the head position test, the preinjection average scores (±SEM) for the rAAV-α-syn and rAAV-GFP groups were +0.5 ± 5.4 and +9.4 ± 2.1 s, respectively. At 3 wk postinjection, i.e., at the time when transgene expression in the AAV-infected cells is fully developed (33–36), the animals in the rAAV-α-syn group showed a marked bias in the direction away from the injected hemisphere (−33.0 ± 5.7 s, as compared with +7.5 ± 2.1 s in the rAAV-GFP group). At 6 wk postinjection, this contralateral bias was reversed to an ipsilateral bias (+17.7 ± 1.7 s), as would be expected from animals with loss of dopamine innervation in the striatum. This bias persisted until the end of the experiment at 16 wk after transduction and was especially strong in two of the three rAAV-α-syn animals (+40.5, +22.3, −14 s, respectively), whereas the rAAV-GFP-injected animals showed no such bias (+5.5 and −7.3 s, respectively).

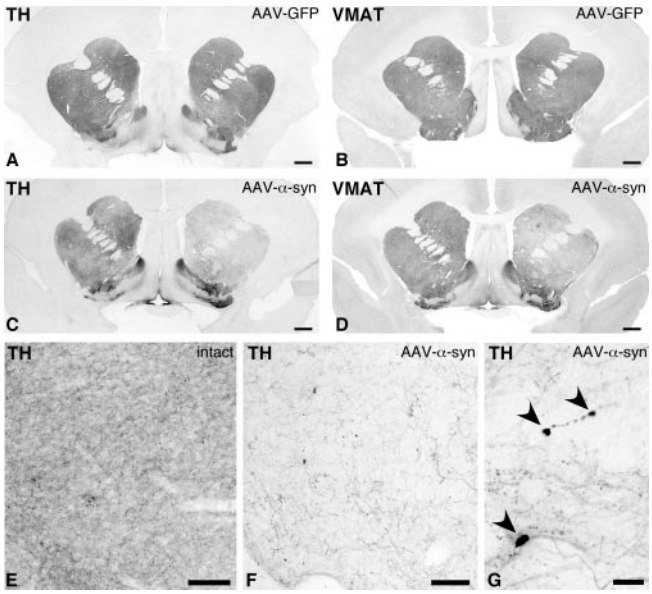

Fig. 4. Photomicrographs illustrating the axonal fiber innervation in the striatum visualized with TH (*A*, *B*, and *E–G*) and VMAT-2 (*B* and *D*) immunohistochemistry. Whereas expression of GFP protein did not alter the density of TH- and VMAT-2-positive fiber innervation in the striatum (*A* and *B*), the expression of α-syn led to prominent loss of fibers both in caudate nucleus and putamen in the transduced hemisphere, as compared with the contralateral intact side (*C* and *D*). Remaining TH-positive fibers in the α-syn-treated animals were sparse (compare *E* and *F*) and contained inclusions (*G*). Scale bars in *A–D* = 1 mm; *E* and *F* = 0.1 mm; *G* = 25 μm.

Discussion

The cellular changes induced by overexpression of α-syn in nigral dopamine neurons reproduces some of the cardinal neuropathological features of human PD, including α-syn-positive cytoplasmic inclusions and α-syn-positive swollen and dystrophic neurites, associated with degenerative changes in TH-positive axons and dendrites. In the rat, this α-synucleinopathy is a slowly developing process that starts at $\approx$3 wk after transduction and is fully developed by 2 mo. At that time point 30–80% of the nigral dopamine neurons and 25–90% of the striatal dopamine innervation are lost. A similar (30–60%) loss of TH- and VMAT-2-positive neurons in the SN, and a 40–50% reduction in TH- and VMAT-2-positive innervation throughout caudate nucleus and putamen was observed in the rAAV-α-syn-treated monkeys. Similar to idiopathic PD, the TH-positive neurons in the VTA and the associated innervation in limbic forebrain regions were relatively spared. These monkeys displayed a type of motor impairment, i.e., head position bias, that is compatible with the observed magnitude of nigral dopamine neuron cell loss. This side bias developed slowly, between 3 and 6 wk after transduction, and was maintained in two of the three animals until the end of the experiment (at 16 wk).

The nigral dopamine neurons seem to be particularly sensitive to α-syn overexpression. Interestingly, however, in both rats and monkeys, part of the transduced dopamine neurons survived long-term without any clear signs of damage, despite a maintained expression of the transduced α-syn protein, whereas others displayed signs of cellular and neuritic pathology suggestive of an ongoing neurodegenerative process. This variable vulnerability may be explained by the observation that α-syn toxicity is closely linked to the level of oxidative stress, and that dopamine neurons may be particularly sensitive due to interaction of α-syn with intracellular dopamine and dopamine-dependent oxidative mechanisms (7, 10, 11, 37, 38). It is worth noting that, with the current technique, the level of transgene expression will vary among the infected cells because neurons close to the injection site may receive more copies of the recombinant virus. However, it is likely that not only the level of α-syn expression but also the level of oxidative stress, which may vary from cell to cell, will determine the impact on the transduced cell. Previous *in vitro* studies (see, e.g., refs. 11, 38, and 39) have shown that the A53T and A30P mutants of human α-syn may be more toxic and make the transduced cells more vulnerable to oxidative stress, than the WT form. In the present model, as in some other *in vivo* experiments (14, 17, 19, 20, 24, 40), both the WT and the A53T mutant α-syn were highly toxic. In the absence of dose-response data, however, we cannot determine whether the two forms may differ in potency.

Neurodegeneration in PD is likely to depend on an interaction between α-syn (and the ubiquitin-proteasome pathway), oxidative stress, and mitochondrial impairment. Current animal models of PD successfully replicate the two latter mechanisms: 6-hydroxydopamine-induced toxicity mediated by oxidative damage, and MPTP- and rotenone-induced toxicity, mediated by chronic inhibition of mitochondrial complex I (1, 41). Targeted overexpression of α-syn in nigral dopamine neurons by rAAV vectors provides a new model of nigrostriatal α-synucleinopathy and α-syn-induced nigrostriatal neurodegeneration that will be a valuable complement to the existing ones. The advantage of this α-synucleinopathy model is that it is chronic and progressive, like human PD, and that it develops neuropathological features, in particular α-syn-positive inclusions and dystrophic neurites, that are similar (although not identical) to those seen in idiopathic PD. Moreover, neurodegeneration and behavioral impairments evolve over a relatively short period, 6–8 wk after transduction as determined in the rat (24), which is advantageous for experimental studies. Compared with standard transgenic mouse technology, vector-mediated transgenesis has a particular attraction, in that the transgenic protein can be delivered to adult animals at any time during the lifespan; that it can be targeted to specific subsets of neurons; that it can be applied uni- or bilaterally, as desired; and that it can be used also in primates. Viral vectors, and the new generation high-titer rAAV vectors in particular, provide new efficient tools for cell-specific, targeted transgenesis in the brain. The feasibility of using this approach in primates, as shown here, opens entirely new possibilities for the generation of transgenic primate models of neurodegenerative diseases, and for *in vivo* studies of pathogenetic mechanisms. Because rAAV vectors can be administered repeatedly to the same cells, they will be interesting also as tools for the expression of genes and intracellular factors that may block or interfere with critical pathogenetic processes (such as formation of toxic fibrils or protein aggregates in rAAV-α-syn-treated animals) and for the exploration of new molecular targets for therapeutic purposes.

We thank Ulla Jarl for expert technical assistance, Lyn Cummings for behavioral observations, the Department of Experimental Psychology at the University of Cambridge for use of the primate facility, the Powell Gene Therapy Center Vector Core Laboratory for production of the vectors, and Dr. Virginia M. Lee and Steven A. Goldman for generous supply of the α-synuclein and Hu antibodies, respectively. This study was supported by grants from the Swedish Medical Research Council (04X-3874 and 99-XG-13285), The Wellcome Trust (to L.E.A.), and the National Institutes of Health (PO1 NS36302, to N.M.).

1. Beal, M. F. (2001) *Nat. Rev. Neurosci.* **2,** 325–334.
2. Dawson, T., Mandir, A. & Lee, M. (2002) *Neuron* **35,** 219–222.
3. Spillantini, M. G., Schmidt, M. L., Lee, V. M., Trojanowski, J. Q., Jakes, R. & Goedert, M. (1997) *Nature* **388,** 839–840.
4. Goedert, M. (2001) *Nat. Rev. Neurosci.* **2,** 492–501.
5. Polymeropoulos, M. H., Lavedan, C., Leroy, E., Ide, S. E., Dehejia, A., Dutra, A., Pike, B., Root, H., Rubenstein, J., Boyer, R., *et al.* (1997) *Science* **276,** 2045–2047.
6. Kruger, R., Kuhn, W., Muller, T., Woitalla, D., Graeber, M., Kosel, S., Przuntek, H., Epplen, J. T., Schols, L. & Riess, O. (1998) *Nat. Genet.* **18,** 106–108.

7. Conway, K. A., Rochet, J. C., Bieganski, R. M. & Lansbury, P. T., Jr. (2001) *Science* **294,** 1346–1349.
8. McNaught, K. S., Olanow, C. W., Halliwell, B., Isacson, O. & Jenner, P. (2001) *Nat. Rev. Neurosci.* **2,** 589–594.
9. Przedborski, S., Chen, Q., Vila, M., Giasson, B. I., Djaldatti, R., Vukosavic, S., Souza, J. M., Jackson-Lewis, V. V., Lee, V. M. & Ischiropoulos, H. (2001) *J. Neurochem.* **76,** 637–640.
10. Xu, J., Kao, S. Y., Lee, F. J., Song, W., Jin, L. W. & Yankner, B. A. (2002) *Nat. Med.* **8,** 600–606.
11. Tabrizi, S. J., Orth, M., Wilkinson, J. M., Taanman, J. W., Warner, T. T., Cooper, J. M. & Schapira, A. H. (2000) *Hum. Mol. Genet.* **9,** 2683–2689.
12. Zhou, W., Hurlbert, M. S., Schaack, J., Prasad, K. N. & Freed, C. R. (2000) *Brain Res.* **866,** 33–43.
13. Junn, E. & Mouradian, M. M. (2002) *Neurosci. Lett.* **320,** 146–150.
14. Feany, M. B. & Bender, W. W. (2000) *Nature* **404,** 394–398.
15. Lee, M. K., Stirling, W., Xu, Y., Xu, X., Qui, D., Mandir, A. S., Dawson, T. M., Copeland, N. G., Jenkins, N. A. & Price, D. L. (2002) *Proc. Natl. Acad. Sci. USA* **99,** 8968–8973.
16. Giasson, B. I., Duda, J. E., Quinn, S. M., Zhang, B., Trojanowski, J. Q. & Lee, V. M. (2002) *Neuron* **34,** 521–533.
17. Masliah, E., Rockenstein, E., Veinbergs, I., Mallory, M., Hashimoto, M., Takeda, A., Sagara, Y., Sisk, A. & Mucke, L. (2000) *Science* **287,** 1265–1269.
18. Matsuoka, Y., Vila, M., Lincoln, S., McCormack, A., Picciano, M., LaFrancois, J., Yu, X., Dickson, D., Langston, W. J., McGowan, E., *et al*. (2001) *Neurobiol. Dis.* **8,** 535–539.
19. Kahle, P. J., Neumann, M., Ozmen, L., Muller, V., Jacobsen, H., Schindzielorz, A., Okochi, M., Leimer, U., van Der Putten, H., Probst, A., *et al*. (2000) *J. Neurosci.* **20,** 6365–6373.
20. van der Putten, H., Wiederhold, K. H., Probst, A., Barbieri, S., Mistl, C., Danner, S., Kauffmann, S., Hofele, K., Spooren, W. P., Ruegg, M. A., *et al*. (2000) *J. Neurosci.* **20,** 6021–6029.
21. Rathke-Hartlieb, S., Kahle, P. J., Neumann, M., Ozmen, L., Haid, S., Okochi, M., Haass, C. & Schulz, J. B. (2001) *J. Neurochem.* **77,** 1181–1184.
22. Samulski, R. J., Sally, M. & Muzyczka, N. (1999) in *The Development of Human Gene Therapy*, ed. Friedmann, T. (Cold Spring Harbor Lab. Press, Plainview, NY), pp. 131–170.
23. Naldini, L. & Verma, I. M. (1999) in *The Development of Human Gene Therapy*, ed. Friedmann, T. (Cold Spring Harbor Lab. Press, Plainview, NY), pp. 47–60.
24. Kirik, D., Rosenblad, C., Burger, C., Lundberg, C., Johansen, T. E., Muzyczka, N., Mandel, R. J. & Bjorklund, A. (2002) *J. Neurosci.* **22,** 2780–2791.
25. Hauswirth, W. W., Lewin, A. S., Zolotukhin, S. & Muzyczka, N. (2000) *Methods Enzymol.* **316,** 743–761.
26. Zolotukhin, S., Byrne, B. J., Mason, E., Zolotukhin, I., Potter, M., Chesnut, K., Summerford, C., Samulski, R. J. & Muzyczka, N. (1999) *Gene Ther.* **6,** 973–985.
27. McLaughlin, S. K., Collis, P., Hermonat, P. L. & Muzyczka, N. (1988) *J. Virol.* **62,** 1963–1973.
28. Xu, L., Daly, T., Gao, C., Flotte, T. R., Song, S., Byrne, B. J., Sands, M. S. & Ponder, K. P. (2001) *Hum. Gene Ther.* **12,** 563–573.
29. Stephan, H., Baron, G. & Schwerdtfeger, W. K. (1980) (Springer, Berlin).
30. Annett, L. E., Rogers, D. C., Hernandez, T. D. & Dunnett, S. B. (1992) *Brain* **115,** 825–856.
31. Annett, L. E., Smyly, R. E., Henderson, J. M., Cummings, R. A., Kendall, A. L. & Dunnett, S. B. (2000) in *Innovative Animal Models of Central Nervous System Disease: From Molecule to Therapy*, eds. Emerich, D. F., Dean, R. L. & Sandberg, P. (Humana, Totowa, NJ), pp. 171–186.
32. West, M. J. (1999) *Trends Neurosci.* **22,** 51–61.
33. Mandel, R. J., Rendahl, K. G., Snyder, R. O. & Leff, S. E. (1999) *Exp. Neurol.* **159,** 47–64.
34. Mandel, R. J., Snyder, R. O. & Leff, S. E. (1999) *Exp. Neurol.* **160,** 205–214.
35. Lo, W. D., Qu, G., Sferra, T. J., Clark, R., Chen, R. & Johnson, P. R. (1999) *Hum. Gene Ther.* **10,** 201–213.
36. Ferrari, F. K., Samulski, T., Shenk, T. & Samulski, R. J. (1996) *J. Virol.* **70,** 3227–3234.
37. Giasson, B. I., Jakes, R., Goedert, M., Duda, J. E., Leight, S., Trojanowski, J. Q. & Lee, V. M. (2000) *J. Neurosci. Res.* **59,** 528–533.
38. Kanda, S., Bishop, J. F., Eglitis, M. A., Yang, Y. & Mouradian, M. M. (2000) *Neuroscience* **97,** 279–284.
39. Ostrerova, N., Petrucelli, L., Farrer, M., Mehta, N., Choi, P., Hardy, J. & Wolozin, B. (1999) *J. Neurosci.* **19,** 5782–5791.
40. Lo Bianco, C., Ridet, J. L., Schneider, B. L., Deglon, N. & Aebischer, P. (2002) *Proc. Natl. Acad. Sci. USA* **99,** 10813–10818.
41. Betarbet, R., Sherer, T. B., MacKenzie, G., Garcia-Osuna, M., Panov, A. V. & Greenamyre, J. T. (2000) *Nat. Neurosci.* **3,** 1301–1306.